# Analysis of the first year's performance of HR Radars in wave measurements and filtered data.

## Technical report N: #04

Version 1.0

Authors: J.Iglesias, G. Llorach-Tó, J. Ballabrera, J. Isern-Fontanet

File: ICATMAR_SO_2024_04_SOCAT_reports_radars.pdf

Date: October 14, 2024

## Abstract

This technical report provides a evaluation of wave data collected by two high-frequency radars (Begur and Creus - ICATMAR) in comparison to a nearby offshore mooring buoy (Cap de Begur - Puertos del Estado) from 2023-03-08 11:00:00 to 2024-06-11 07:00:00. Results show a low correlation between the HF radar and buoy measurement systems using raw data, but a significant improvement is observed once the data is filtered using the parameters provided by the radar. Currently, the wave data from the HF radars is not reliable for operational wave detection, but the data can be used if supervised.

# 1 Introduction

Monitoring ocean waves is crucial for several fields. From fisheries management to maritime safety, real-time wave monitoring serves as an early warning system for potential hazards such as rough seas, high swells, or abrupt changes in wave patterns. Additionally, in infrastructure management, understanding wave behavior is essential for preempting and mitigating potential damages to coastal structures, ports, and offshore platforms. Moreover, ocean wave monitoring enhances our understanding of marine dynamics, including phenomena like climate change impacts, oceanic circulation patterns, and coastal erosion processes (Saviano et al. (2019)). Furthermore, robust wave monitoring systems increase the availability of data for assimilation into numerical models and forecasting tools (Toste et al. (2024)).

ICATMAR (ICATMAR (2024)) has recently installed several HF radars along the Catalan Coast. The primary objective of the HF radars is to measure sea water velocities at the surface level. As a secondary function, under specific conditions, these HF radars can also provide measurements of significant wave height, mean wave period, mean wave direction, and wind direction (Lipa et al. (2022)). Since these measurements are inferred from the HF radar signal, they need to be validated against other measurement systems.

The NW Mediterranean sea contains unique characteristics, the continental shelf is narrow (5 to 18 kilometers on average) and crossed by submarine canyons. The shelf-slope front separates waters of different densities between the continental shelf and the open sea. This front favors the narrowing of the northern current, which comes from the Gulf of Lion when it reaches the Catalan coast and circulates in a southwesterly direction along the continental shelf. In this space, there are two differentiated divergence zones, one towards the point 42 ºN, 4 ºE and the other around the point 41 ºN, 3 ºE (Pinot et al. (1995); Millot (1999)). Figure 1 shows the region of interest, accompanied by corresponding bathymetry data, highlighting the mentioned zone. The predominant winds come from the North and Northwest, primarily during December and January. Southerly and Easterly winds are also important particularly during the months of February, March, April and November (del Amo, 2000).

The radar measuring network will include seven HF radar stations (Cap de Creus, Cap de Begur, Tossa de Mar, Arenys de Mar, Barcelona, Port Ginesta, and Port Segur - Calafell). This network could be complemented by the HF radar network of the RIADE project, which comprises three operational HF radar stations (Cap Salou, Alfacada, and Port of Vinaròs) currently operated by Puertos del Estado. It is estimated that the network will have an approximate range of 80 km offshore from the coast, although the range is influenced by the final location of the antennas. For example, at Cap de Creus, the range is estimated to be 60 km due to signal attenuation with increasing distance from the sea. This combined network would provide continuous coverage from the north of Cap de Creus to the Ebro Delta. The integration of both networks would also offer superior coverage, particularly due to the synergy between the radars at Port Segur - Calafell (XarxaHFCat) and the radars at Cap Salou and Alfacada (RIADE), as shown in Table 1. In this report, only the Begur and Creus HF radar data will be analyzed.

The data processed by the CODAR software have been analyzed in this report. This data includes a value for significant wave height ($Hs$) per radar and time, which is averaged over time and space as described in the data section. Additionally, values for wave direction and period are provided by the software. Since $Hs$ is the most crucial parameter for various applications such as safety and navigation, a more comprehensive analysis of this variable will be conducted. The analyzed period was omitted from this report because the extracted information does not differ from what is already presented for $Hs$ or wave direction.

Table 1: Total estimated coverage according to the HF radar network.

| HF RADAR NETWORK | ESTIMATED COVERAGE ($km^2$) |
|---|---|
| HF Radar System of the RIADE Project | 8,283 |
| Catalan HF Radar Network (XarxaHFCat) | 21,085 |
| Combination of both networks | 30,407 |

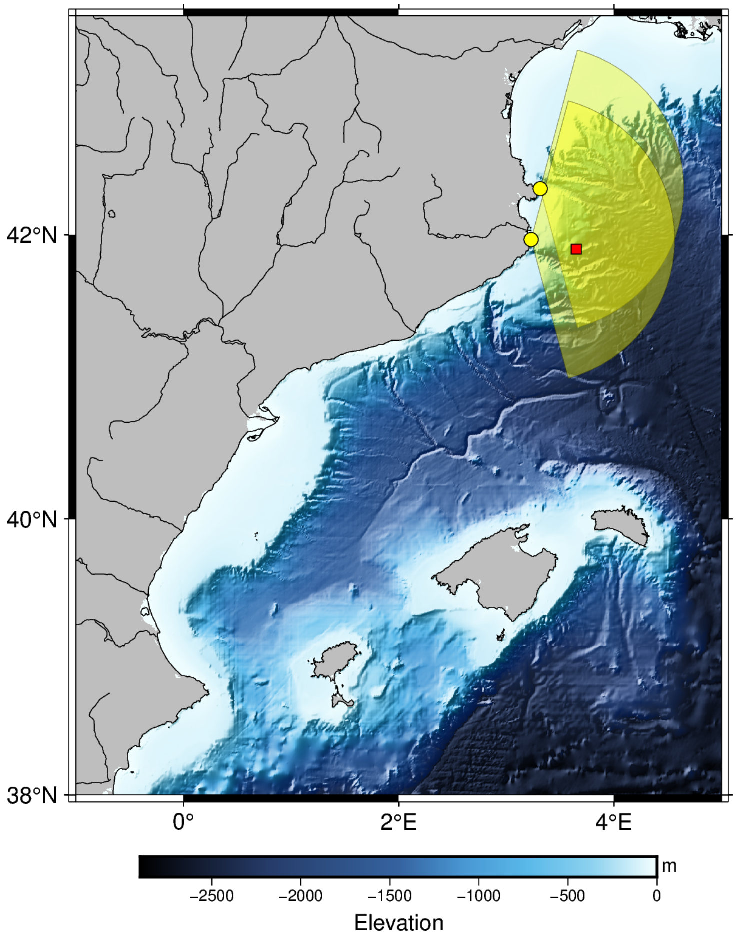


Figure 1: The NW Mediterranean sea along with HF radars (●) of Begur and creus, and mooring buoy location (■).

## 2 Data, instruments and limitations

## 2.1 HF radars

### Coastal Ocean Dynamics Applications Radar (CODAR) description

CODAR operates using sky transmission of waves in the high-frequency (HF) band at 13.5 MHz in XarxaHFCat radars. These electromagnetic waves have wavelengths similar to wind-driven gravity waves on the ocean surface. When a high-frequency signal reaches the ocean's rough surface, a portion of the energy is scattered back towards the source, and the receiver measures this reflected signal. This backscattering produces an energy spectrum at the receiver, even from a single-frequency source, due to the sea surface's shape and motion. Interpreting these spectral returns for various transmit frequencies is key to extracting ocean information and measuring surface currents. In this report, the significant wave height ($Hs$) is studied. $Hs$ is the average of the highest one-third of observed waves.

In addition to the strong echo used for measuring currents, a weaker but still usable echo at shifted Doppler frequencies is sometimes observed in the returned signal. These shifted Doppler echoes are sidebands resulting from the rotation of shorter Bragg-scattering waves riding on top of the longer underlying waves. The strengths and shapes of these echo sidebands are analyzed to extract information about waves.

To obtain significant wave height from CODAR data, second-order radar spectrum generated by pairs of ocean waves interacting with radar signals is obtained. This spectrum can be described by a two-dimensional integral equation that incorporates the antenna pattern, coupling coefficient, and ocean wave spectra. The Pierse-Moscovich model is applied to simplify this process; this model helps in relating radar measurements to ocean wave properties. Additionally, by examining all radar frequencies, one can retrieve the Fourier directional coefficients of the ocean wave spectrum across all ocean wave frequencies, effectively obtaining the complete spectrum.

The mean-square wave height is determined by integrating the non-directional coefficient of the temporal wave spectrum over frequency. Consequently, the significant wave height is approximately three times the square root of this integral.

For the wave solutions to remain valid, there is a limit on the wave height that can be accurately measured at a given frequency. If the sea state surpasses this limit, the second-order radar spectrum begins to saturate, leading to an underestimation of the predicted ocean wave height. The mathematical theory can be found at Lipa and Barrick (1986).

### CODAR specifications and limitations

The HF radar (CODAR) provides wave data every 10 minutes. The wave measurement is taken from a specific arc area in front of the radar (range cell). The wave measurement provided by the HF radar corresponds to a temporal and spatial average. The distance between the HF radar wave measurement and the buoy depends on the range cell. The wave data variables utilized in this report are: significant wave height, mean wave period, and mean wave direction.

The radars utilize Doppler frequency shifts, specifically the second-order peak, to derive wave characteristics. However, it is essential to note that this feature is secondary within the radar's functionality, which implies certain limitations such as:

- Strong currents cause distortion in the measurement.

- Wave signal is not present for small waves.
- Wave height measurements have an upper limit (8 meters for HF radars operating at 13.5 MHz, as the ones in this report).

The availability of wave data from the HF radar system depends on the software's interpretation of the HF signal, which might not always be sufficient to extract wave data at a given time. It is common to have missing data points on the 10-minute time scale. In some studies, such as Vesecky and Laws (2010), the spectrum is filtered before processing the data for ship detection. Other studies, like Lorente et al. (2022), provide guidelines and techniques to filter the data and highlight the weaknesses of HF radars in terms of data reliability. In this report, only the data provided by CODAR's software (MUSIC, acronym of MUltiple SIgnal Classification) will be analyzed, and various methodologies will be considered to improve the data in the future.

### Metadata description

Several parameters can be found in the header of the document generated by CODAR software, some related to timestamp, data coverage, transmission frequencies, etc. The most important ones for determining data quality are explained here. The wave values are defined from several spectra (CSS). For the XarxaHFCat radar network, an average of 7 CSSs is used to generate output every 10 minutes, with a 15-minute averaging period. The obtained wave vectors undergo a filtering process in CODAR, resulting in each row of the wave data files. A key reference value is the Spectra Count, representing the number of range cells (RC) multiplied by the number of CSSs (7 for XarxaHFCat), yielding a Spectra Count range of 0 to 168. Higher Spectra Counts indicate better data quality. For Doppler bins in XarxaHFCat, a spectrum has up to 512 bins (256 positive and negative), but only those in the 2nd order region are used for wave and current determination. The Vector Flag indicates the status of each vector: 0 means normal, and specific flags (e.g., 496, 368) denote issues like insufficient 2nd order Doppler points or significant changes in wave height or period. Height Valid Points, indicating the number of vectors used by the filtering application, correlate with data quality, with good wave results typically needing 15-30% of the Spectra Count. This 5 parameters (doppler bins, vector flag, height valid points, range cell and spectra count) were used to filter the data provided by the CODAR as a quality control. Few more details can be found at section 7.

## 2.2 Mooring buoy description

The buoy's specifications utilized in this technical report have the following characteristics:

- Longitude 2.2ºE.
- Latitude 41.32ºN.
- Depth of 68m.
- Directional Triaxis sensor.

This instrument, equipped with directional wave sensors (WaveScan type buoy) gathers hourly data and measures a series of instantaneous elevations over the sea surface for a duration of minutes (typically around 20 minutes, though this duration may vary depending on the buoy). Following data collection, parameters such as significant wave height ($H_s$), mean wave period, mean wave direction, etc., are standardized to a zero value and undergo spectral analysis before being transmitted.

## 2.3 Methodology

The measurements from Begur and Cap de Creus are compared with data from a meteo-oceanographic buoy located near Begur. The buoy data are interpolated from hourly to ten-minute intervals to align with the frequency of radar measurements.

It's important to note that the mooring buoy and the Begur radar are separated by a distance of 36 kilometers, while the mooring buoy and the Cap de Creus radar are 54 kilometers apart, the radars only have 15 range cells in wave measurements, which corresponds to a maximum value of 25 kilometers approximately. Notably, the Cap de Creus radar is considerably farther from Begur than the Begur radar, and this distance may affect the representativeness of the radar-derived significant wave height data compared to the buoy's location.

The CODAR data contains numerous invalid values that require filtering. For this initial analysis, an initial filter based on the vector flag has been applied to discard all values reported as problematic by the radar as explained above. Subsequently, a permutation of the four variables (height valid points, Doppler bins, spectra count, and range cell) was conducted. This process aimed to compute metrics such as the Root Mean Square Difference (RMSD) between wave heights provided by the radar and those from the buoy, absolute differences grouped by thresholds (0.25m, 0.5m, 1m, and 2m), and the number of discarded points. The objective was to align radar values closely with buoy measurements while minimizing the number of discarded points. Additionally, significant deviations from buoy data were penalized.

It's crucial to not solely rely on RMSD, it tends to penalize outliers, but due to the large dataset size, instances where radar records extreme wave heights exceeding 8m alongside values just centimeters high can still be retained. This discrepancy highlights the need for additional analysis of these cases separately by means of another parameters.

Finally, from over 1,000,000 values analyzed at each location, the parameters of table 2 have been selected for detailed evaluation. This table shows the minimum selected value, since these are parameters where a higher number indicates better data quality, filtering has only been applied at the lower limit. The max. value is the maximum available value.

Table 2: Table of selected (minimum values) for data quality control as well as their maximum available value.

| Parameters | Begur | | Creus | |
|---|---|---|---|---|
| | **Min. value** | **Max. value** | **Min. value** | **Max. value** |
| Height valid points | 12 | 96 | 2 | 77 |
| Doppler bins | 6 | 26 | 4 | 26 |
| Spectra count | 9 | 98 | 29 | 98 |
| Range cell | 7 | 15 | 5 | 15 |

# 3 Results and discussion

## 3.1 Raw data provided by CODAR software

The data presented in Annex A, figure 6 consists of time series separated by months, showcasing information available without applying additional filters beyond those already applied by the CODAR software. Instances where the software does not meet quality control standards result in gaps within the time series. These datasets exhibit several issues, including a notable amount of missing data: 21,636 values at Begur and 28,985 values at Creus, equivalent to 32.6% and 43.7% of the total expected data points if collected every 10 minutes during the study period. Furthermore, these data occasionally deviate from the trends observed at the mooring buoy. In some cases, abnormally large values are recorded, such as instances where $Hs$ reaches up to 8m despite the measured $Hs$ being less than 30cm, as specified in radar limitations.

## 3.2 Filtered data analysis

As explained in Section 2.3 only data meeting quality control parameters (table 2) will be analyzed from this point onward; the rest was deleted and appear as gaps.

### $Hs$ comparison

Figure 2 shows $Hs$ values of the mooring buoy (**black**) and radars of Begur (**blue**) and Creus (**cyan**) segmented by month over the study period. The figure is divided into sections to facilitate clearer observation of results, with eliminated values represented in a lighter color and marked with a cross. This visualization is crucial for understanding the impact of data filtering. Despite significant gaps in the time series, the remaining data generally aligns closely with mooring buoy values. Furthermore, most of the outliers that significantly differ from the reference data have been effectively removed. This $Hs$ from HF radar data is more similar to the one of the mooring buoy (or reference).

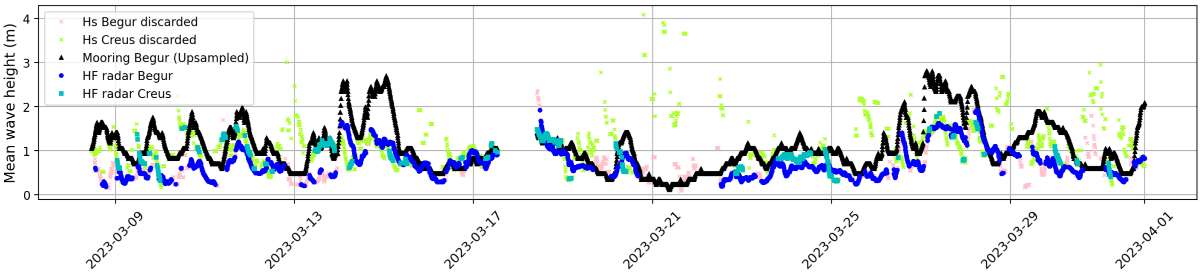


Figure 2: Comparison of significant wave height ($H_s$) data in Begur: mooring buoy (▲) versus radar data from Begur (●) and Creus (■), with discarded Begur (×) and Creus (×) data.

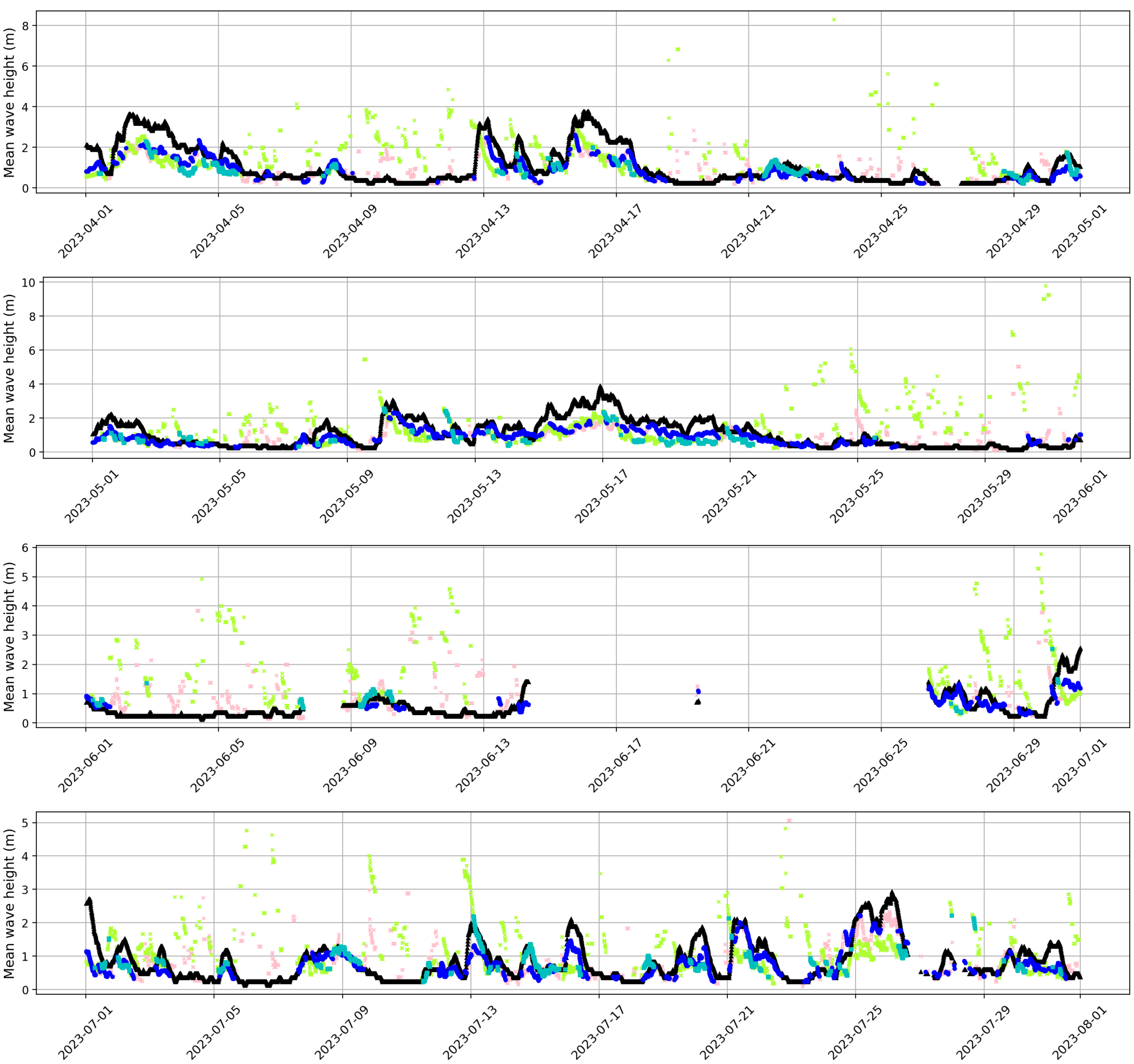

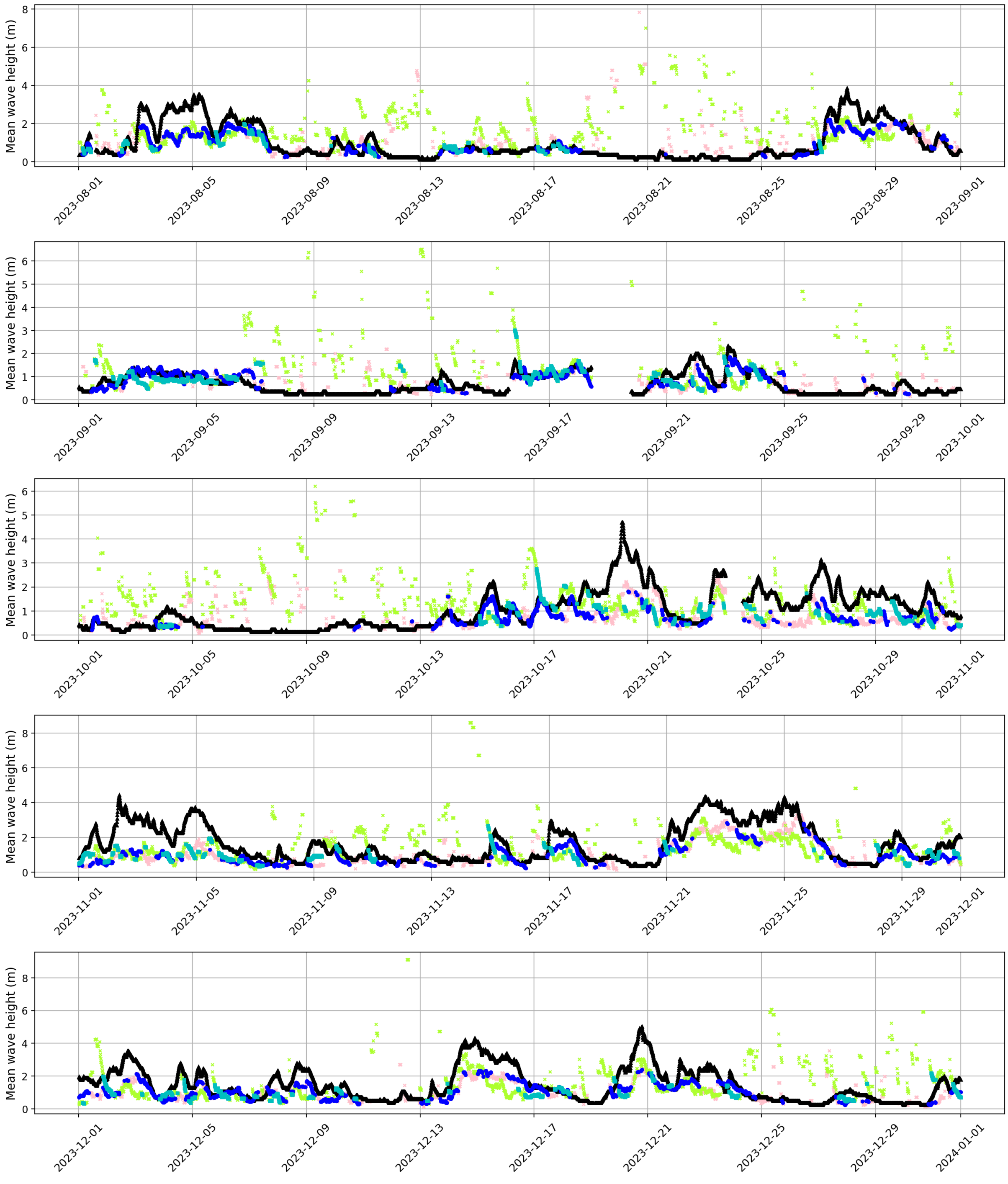
Mean wave height (m)
2023-08-01
2023-08-05
2023-08-09
2023-08-13
2023-08-17
2023-08-21
2023-08-25
2023-08-29
2023-09-01
Mean wave height (m)
2023-09-01
2023-09-05
2023-09-09
2023-09-13
2023-09-17
2023-09-21
2023-09-25
2023-09-29
2023-10-01
Mean wave height (m)
2023-10-01
2023-10-05
2023-10-09
2023-10-13
2023-10-17
2023-10-21
2023-10-25
2023-10-29
2023-11-01
Mean wave height (m)
2023-11-01
2023-11-05
2023-11-09
2023-11-13
2023-11-17
2023-11-21
2023-11-25
2023-11-29
2023-12-01
Mean wave height (m)
2023-12-01
2023-12-05
2023-12-09
2023-12-13
2023-12-17
2023-12-21
2023-12-25
2023-12-29
2024-01-01

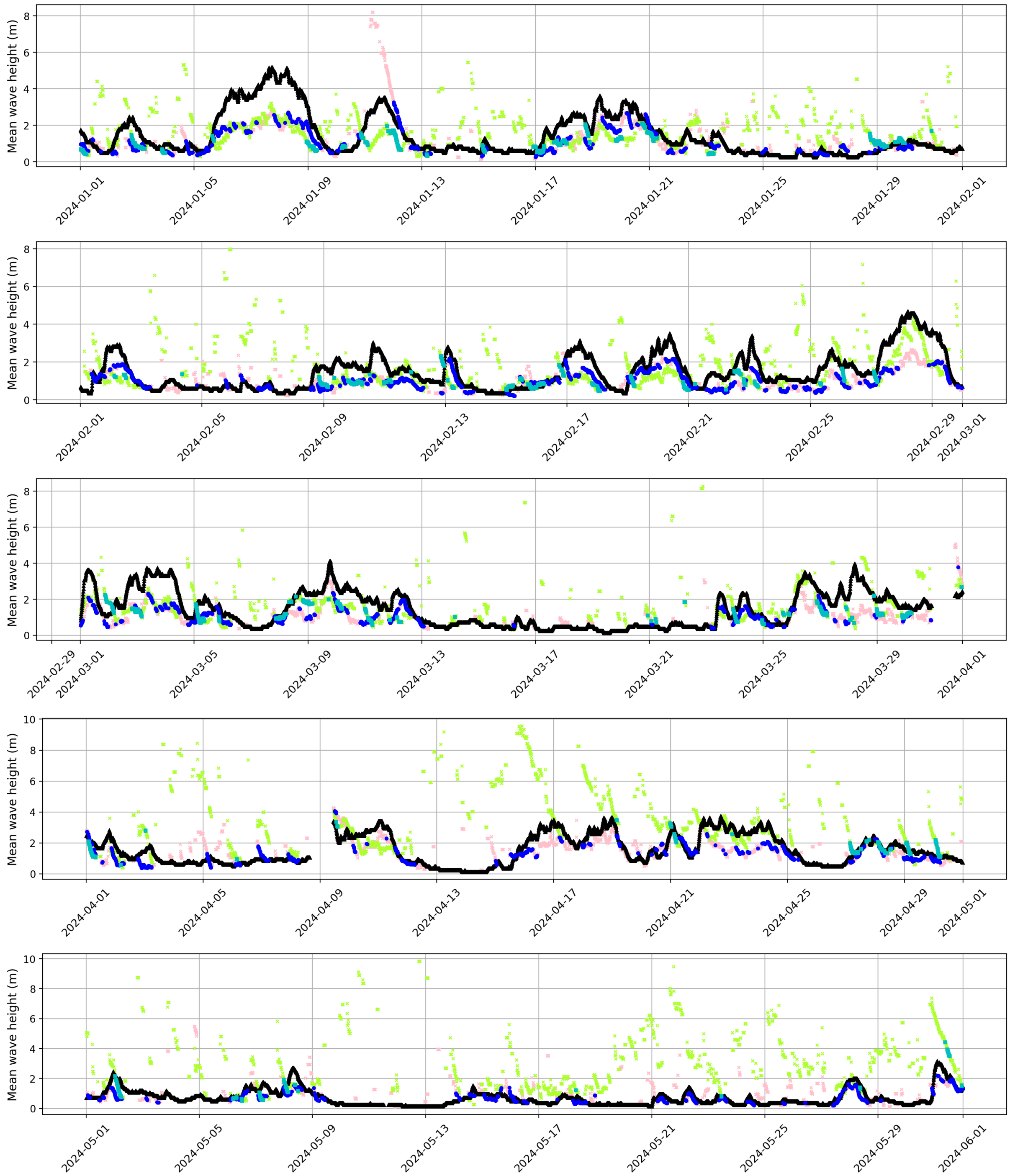
Mean wave height (m)
2024-01-01 2024-01-05 2024-01-09 2024-01-13 2024-01-17 2024-01-21 2024-01-25 2024-01-29 2024-02-01
Mean wave height (m)
2024-02-01 2024-02-05 2024-02-09 2024-02-13 2024-02-17 2024-02-21 2024-02-25 2024-02-29 2024-03-01
Mean wave height (m)
2024-02-29 2024-03-01 2024-03-05 2024-03-09 2024-03-13 2024-03-17 2024-03-21 2024-03-25 2024-03-29 2024-04-01
Mean wave height (m)
2024-04-01 2024-04-05 2024-04-09 2024-04-13 2024-04-17 2024-04-21 2024-04-25 2024-04-29 2024-05-01
Mean wave height (m)
2024-05-01 2024-05-05 2024-05-09 2024-05-13 2024-05-17 2024-05-21 2024-05-25 2024-05-29 2024-06-01

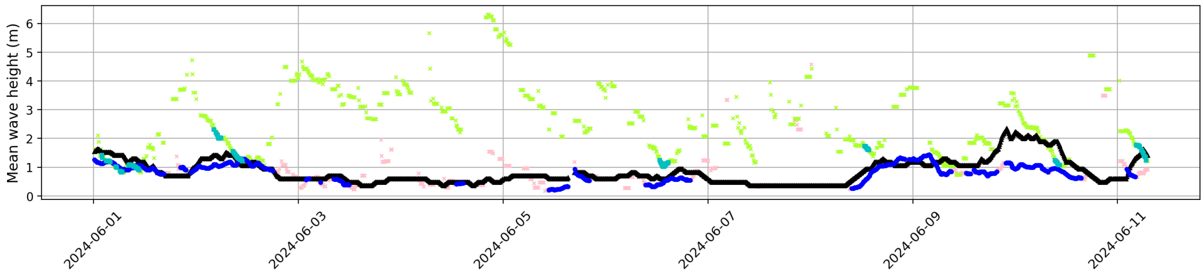


To visualize the differences and their relationship with the magnitude of $Hs$ in a straightforward manner, a boxplot of the discrepancies between the two radars and the mooring buoy was employed (Figure 3). In this boxplot, the data is segmented into different bins corresponding to the $Hs$ measured by the mooring buoy. The differences between each radar and the buoy are then depicted, accompanied by the count (n) of occurrences within each bin. For instance, at Cap de Creus, there are only 3 instances where the $Hs$ magnitude falls between 4.00m and 5.16m, with the filtered data.

Overall, the graph demonstrates that as the mooring-measured $Hs$ increases, the differences tend to enlarge, while the number of outliers, calculated using Seaborn Waskom (2021), diminishes. It can also be observed that, in general, the radar tends to underestimate $Hs$, except for outliers, which are typically overestimated.

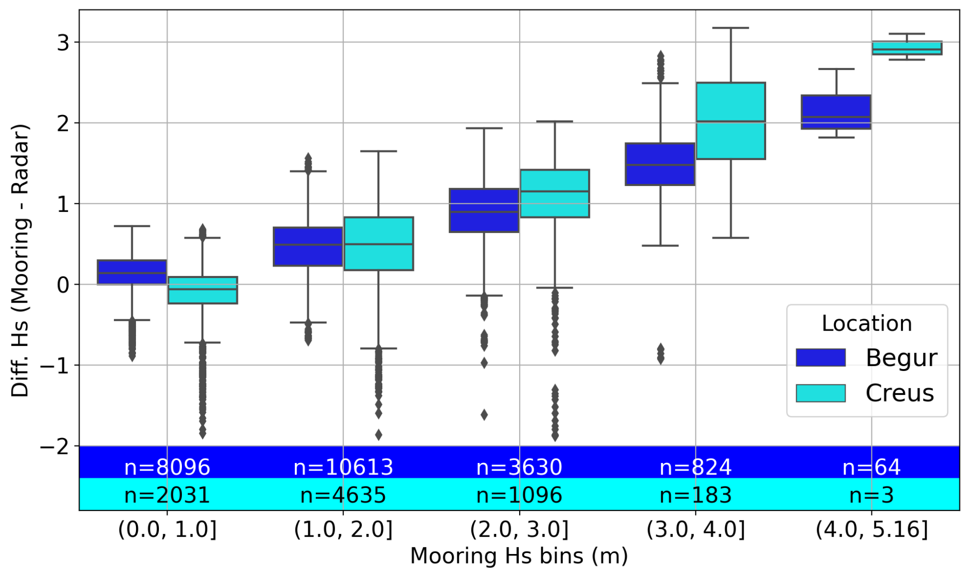


Figure 3: Boxplot of difference $H_s$ measured by the buoy and the HF radar binned by $H_s$ magnitude using mooring buoy as a reference in Begur, n is the number of observations.

Additionally, the correlation between the two radars and the mooring has been calculated, resulting in values of 0.787 and 0.346 in Begur and Creus, respectively. This values of correlation are only qualitative since the data contain nans that affects the temporal series.

In Figure 4, the directional roses of the three observations being compared can be seen. These results show significant similarity between the two located in Begur, but there is considerable difference with the Creus area.

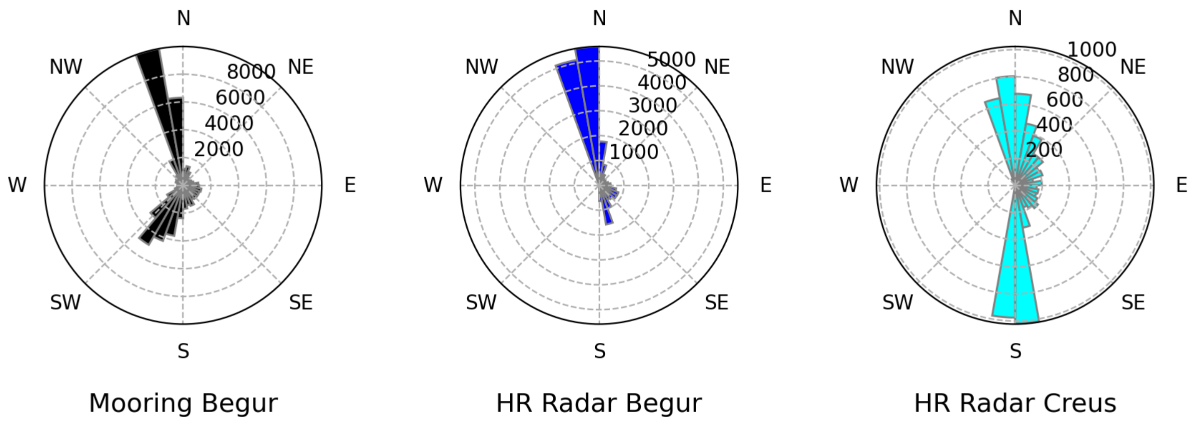


Figure 4: Wave direction comparion in Begur and Creus radar and Begur mooring observations.

Figure 5 shows the density scatter plot between the mooring and CODAR. In the case of Begur, a correlation coefficient of 0.79, a slope of 0.5, and an offset of 0.24 can be observed. Therefore, it is evident that the radar is underestimating most values. This regression line would not be suitable for radar calibration due to significant dispersion among points.

Looking at the Creus data, the correlation coefficient, slope, and intercept are 0.35, 0.23, and 0.65, respectively. Thus, it is clearly a worse case compared to Begur, with even greater dispersion observed in this scenario.

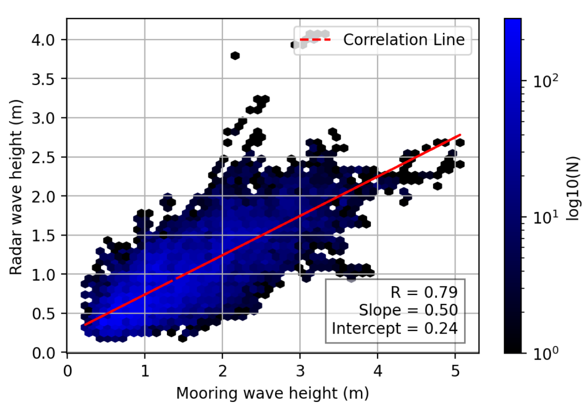


(a) Density scatter plot Begur

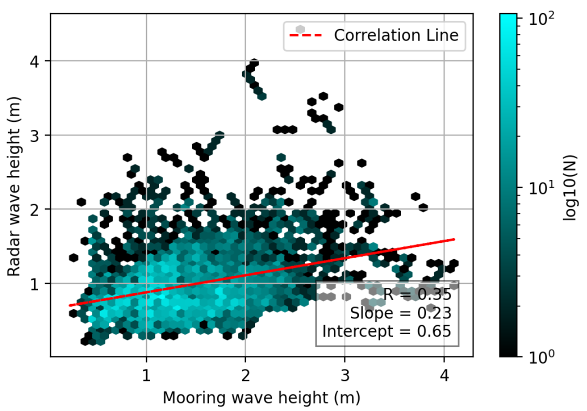


(b) Density scatter plot Creus

Figure 5: Comparison of density scatter plots

# 4 Conclusions

In general, radars often struggle to accurately measure significant wave heights compared to nearby buoys. Their limitations becomes evident, especially for extreme wave values when the actual ones are low. Despite applying filtering parameters, improvements are only modest, with root mean square differences of 0.655 meters in Begur and 0.767 meters in Creus. These values are still insufficient for rigorous scientific studies.

It's important to note that mooring buoys provide localized wave data influenced by specific local conditions, whereas radar data reflects a broader average of wave activity. For radar's wave prediction capability to be reliable, rigorous quality control of radar data is essential.

# 5 Future work

The objective of this study was to analyze and compare the data with the buoys of Begur. As seen in the conclusions, the data is not suitable for an operational model or for data assimilation in numerical CFD models. One part of the analysis, not included in this study, is the exploration of artificial intelligence methods for quality control. The objective was to classify the significant wave height values into different categories corresponding to the ranges of difference with the mooring corresponding to "<=0.5", "<=1", "<=2", ">2" meters using only: wave NF, vector flag, wave method, valid points, and standard deviation parameters. Through software Matlab and Weka achieved a 70% correct classification accuracy. This approach explored random forest, KNN, SVM, and other models and techniques for data quality control, which will be further studied in detail. If satisfactory results are obtained, they will be included in future technical reports.

# 6 Annex A

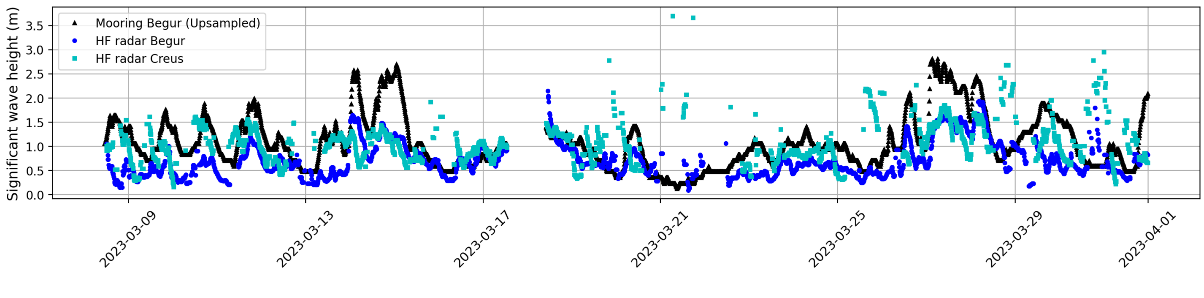


Figure 6: Comparison of significant wave height ($H_s$) data in Begur: mooring buoy (▲) versus radar data from Begur (●) and Creus (■), unfiltered data.

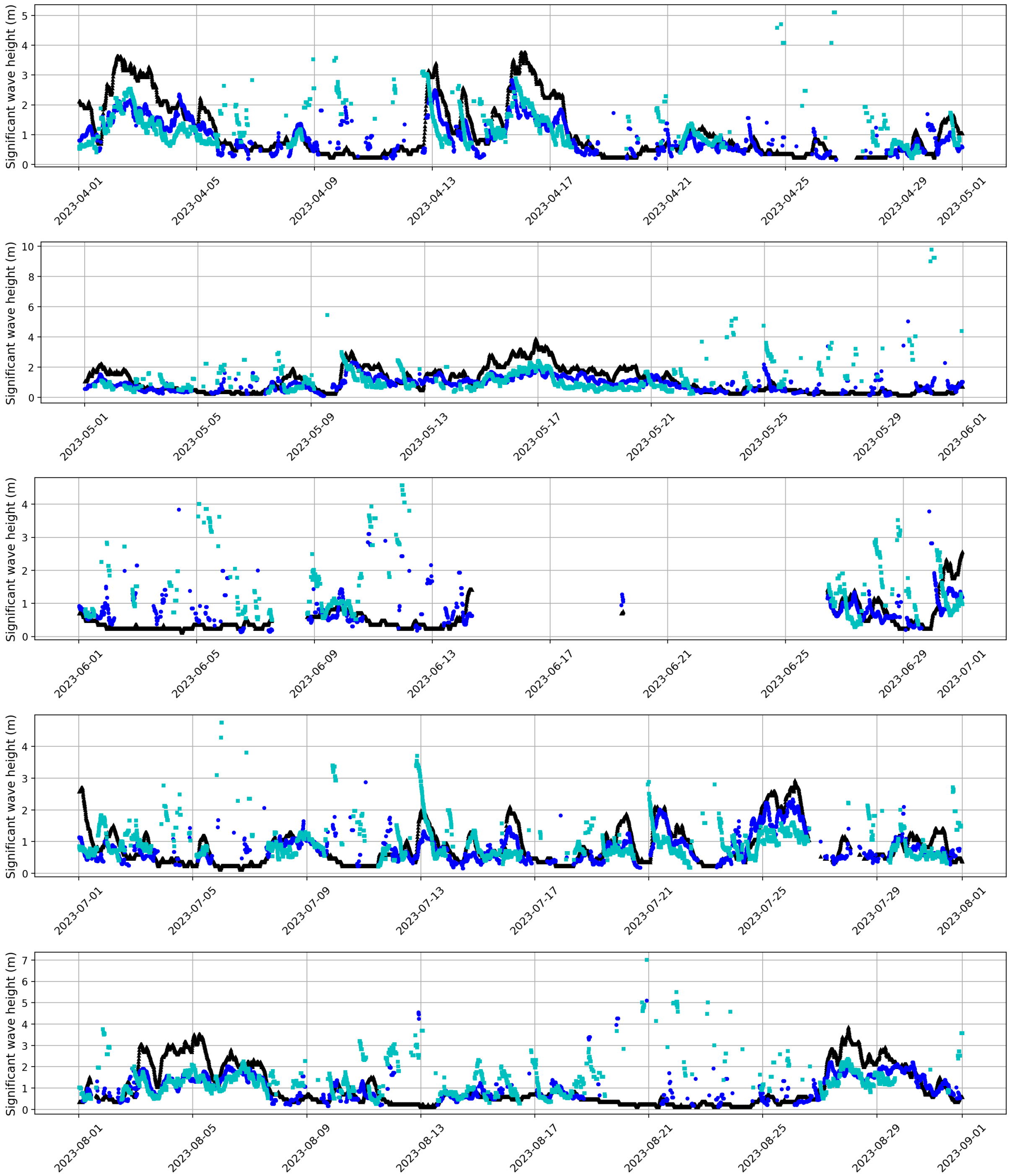
Significant wave height (m)
2023-04-01
2023-04-05
2023-04-09
2023-04-13
2023-04-17
2023-04-21
2023-04-25
2023-04-29
2023-05-01
Significant wave height (m)
2023-05-01
2023-05-05
2023-05-09
2023-05-13
2023-05-17
2023-05-21
2023-05-25
2023-05-29
2023-06-01
Significant wave height (m)
2023-06-01
2023-06-05
2023-06-09
2023-06-13
2023-06-17
2023-06-21
2023-06-25
2023-06-29
2023-07-01
Significant wave height (m)
2023-07-01
2023-07-05
2023-07-09
2023-07-13
2023-07-17
2023-07-21
2023-07-25
2023-07-29
2023-08-01
Significant wave height (m)
2023-08-01
2023-08-05
2023-08-09
2023-08-13
2023-08-17
2023-08-21
2023-08-25
2023-08-29
2023-09-01

## 6. ANNEX A

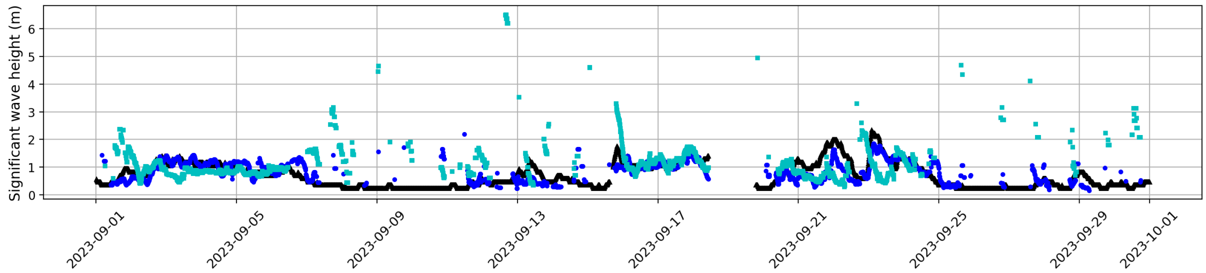
Significant wave height (m)
2023-09-01
2023-09-05
2023-09-09
2023-09-13
2023-09-17
2023-09-21
2023-09-25
2023-09-29
2023-10-01

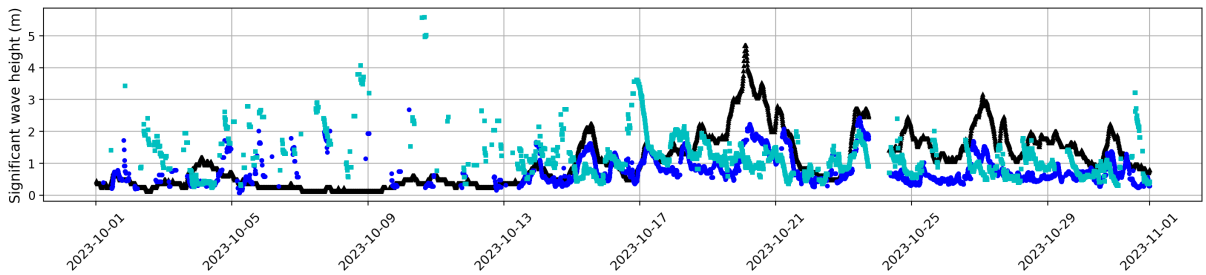
Significant wave height (m)
2023-10-01
2023-10-05
2023-10-09
2023-10-13
2023-10-17
2023-10-21
2023-10-25
2023-10-29
2023-11-01

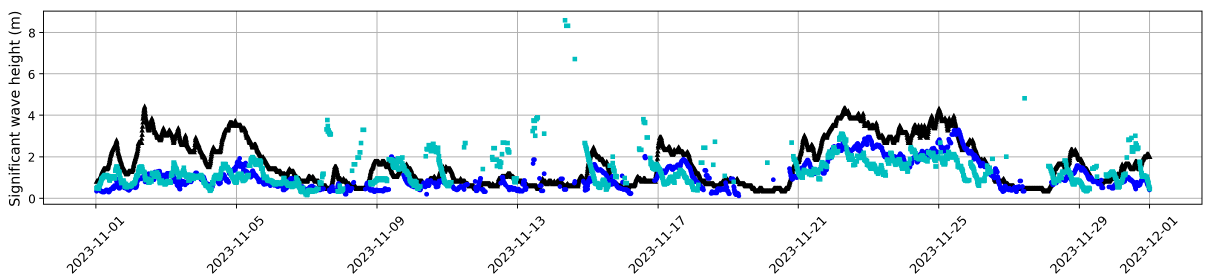
Significant wave height (m)
2023-11-01
2023-11-05
2023-11-09
2023-11-13
2023-11-17
2023-11-21
2023-11-25
2023-11-29
2023-12-01

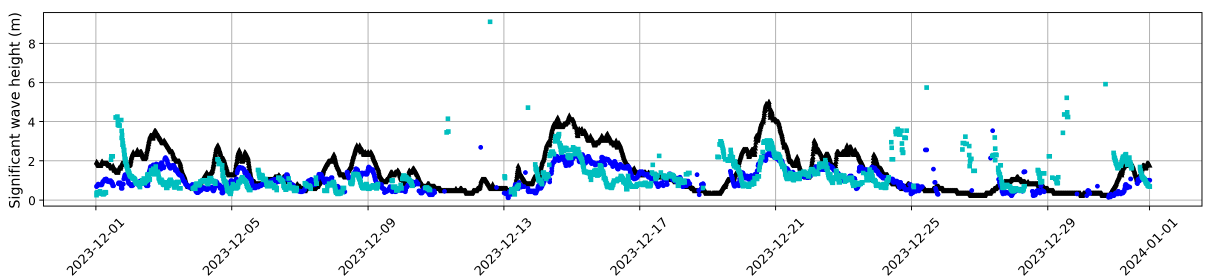
Significant wave height (m)
2023-12-01
2023-12-05
2023-12-09
2023-12-13
2023-12-17
2023-12-21
2023-12-25
2023-12-29
2024-01-01

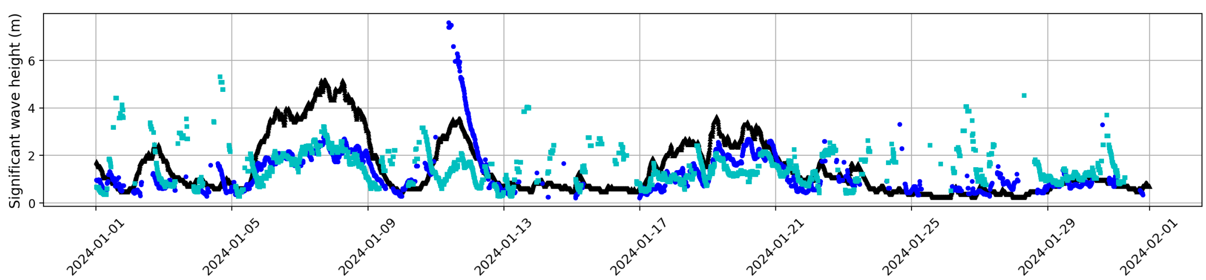
Significant wave height (m)
2024-01-01
2024-01-05
2024-01-09
2024-01-13
2024-01-17
2024-01-21
2024-01-25
2024-01-29
2024-02-01

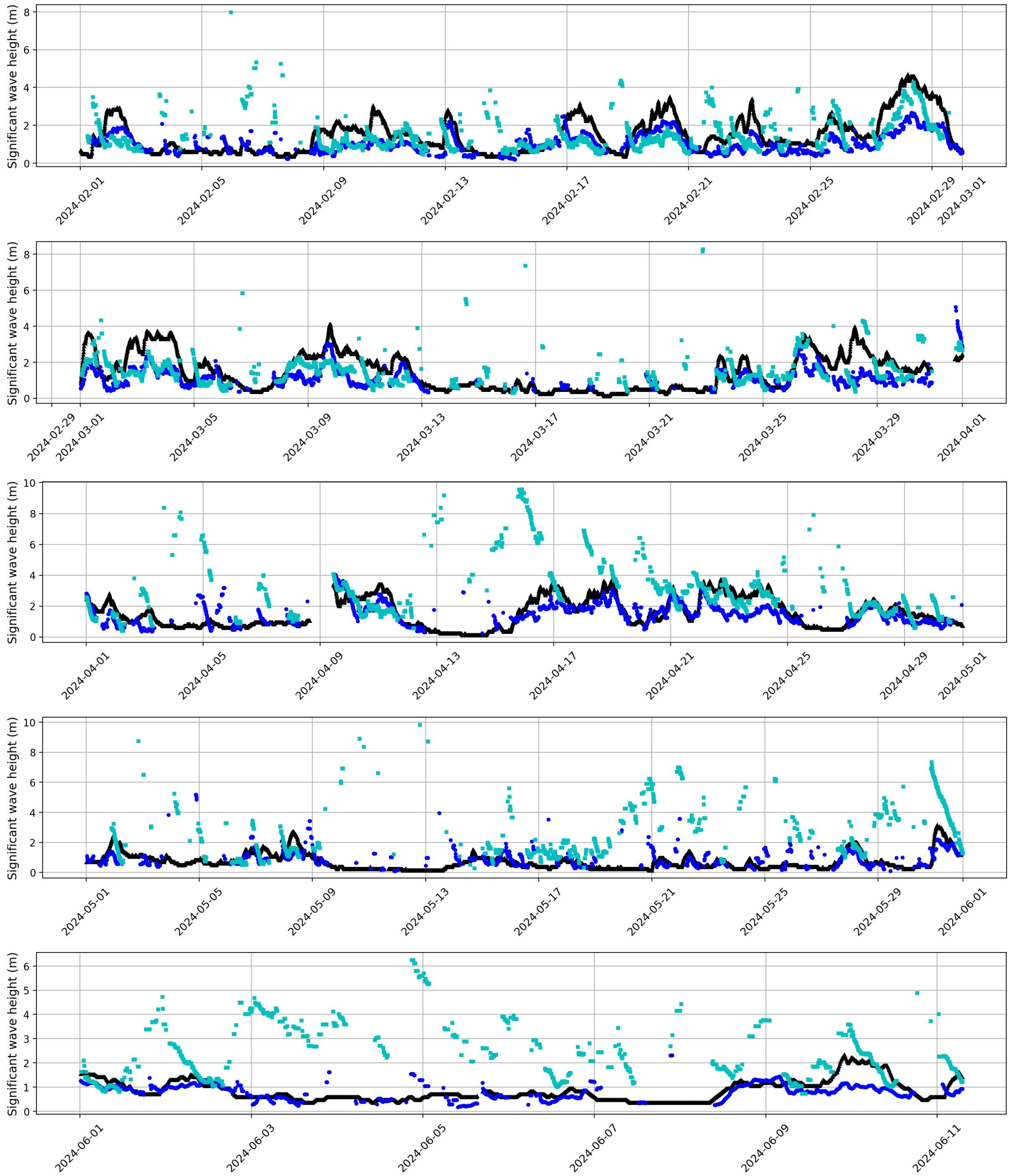


# 7 Annex B

This section describes the methodology of MUSIC software to obtain the wave from CODAR.

# 7. ANNEX B

The CODAR radar ( formed by 3 radars) emits waves that travel over the sea and receives a spectrum called CSQ, which reflects the current state of the sea at a given moment. Every seven CSQ spectra are averaged, and then a noise filter is applied to remove interference from sources like ships. This process generates a called "CSS" file every 10 minutes.

Figure 7, is an example of this spectrum, where each horizontal line represents a range cell, which is a circular arc with a specific radius, with the radar at the center and the resolution of these range cells is 1.664 km, and the vertical lines represent Doppler bins, indicating the frequency range used to analyze currents and waves.

Each radar measures the wave parameters such as significant wave height, wave period, and the direction of both waves and wind for each range cell. However, these values are only calculated if there is enough energy reflected from the sea. In distant range cells, wave data often cannot be calculated due to insufficient reflected energy.

The direction of the waves is determined by observing the peaks between the first and second orders of the Doppler shift, in both the positive and negative regions.

Each CSQ obtains data from three different spectra (loop 1, loop 2, and loop 3), one for each of the three antennas it has. Therefore, each spectrum is visualized with three separate graphs, corresponding to the three antennas.

Finally, the selected range cell selected from MUSIC software and analized in this technical report is the one that shows the cleanest data, with minimal interference, consistency, and no significant changes.

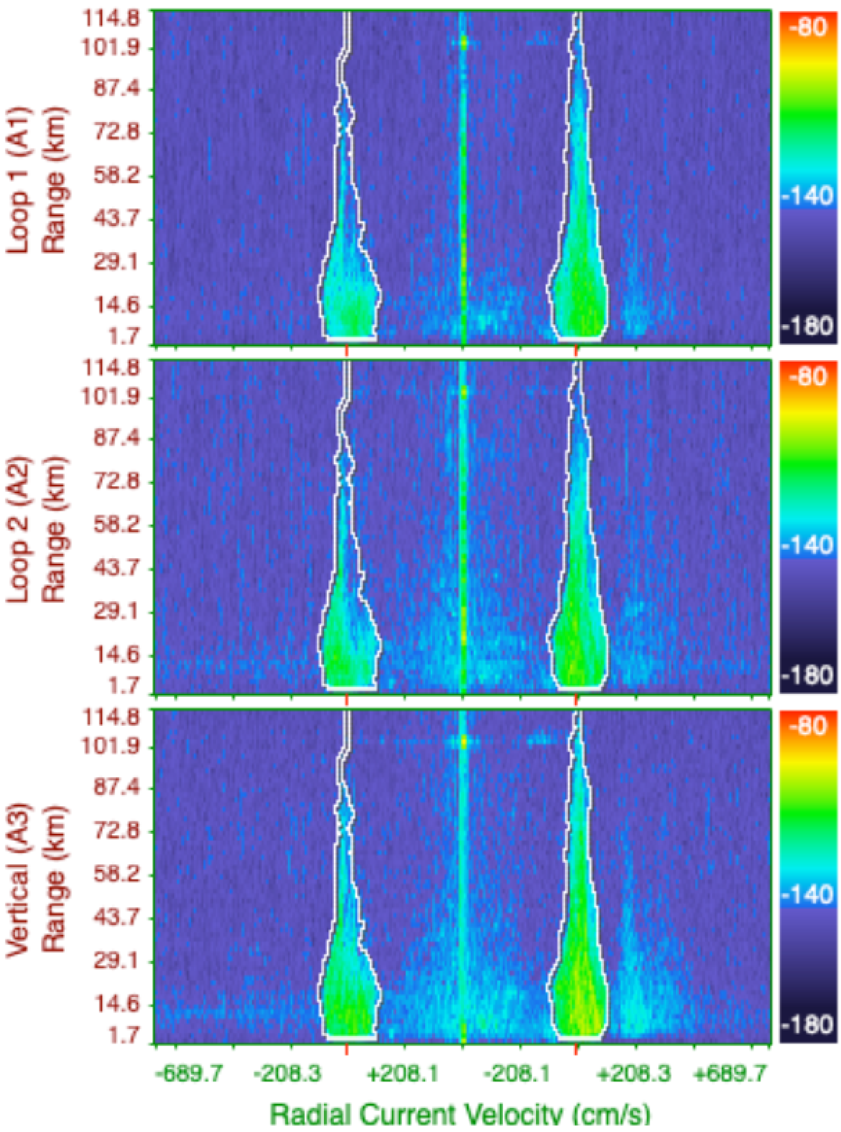


Figure 7: Spectra loop example of XarxaHFCat radar CSQ showing the spectra of the three radars that compose a single CODAR.

# Bibliography


del Amo, P. A. A. (2000). Aspectos de la variabilidad de mesoescala de la circulación marina en la plataforma continental catalana. PhD thesis, Universitat Politècnica de Catalunya (UPC).

ICATMAR (2024). Icatmar - institute of coastal and marine research. https://icatmar.cat/en/. Accessed: 2024-07-08.

Lipa, B., Daugharty, M., Losekoot, M., and Fernandes, M. (2022). Progress in compact hf radar measurement of bimodal ocean wave parameters. Remote Sensing, 14(11):2631.

Lipa, B. J. and Barrick, D. E. (1986). Extraction of sea state from hf radar sea echo: Mathematical theory and modeling. Radio Science, 21(1):81–100.

Lorente, P., Aguiar, E., Bendoni, M., Berta, M., Brandini, C., Cáceres-Euse, A., Capodici, F., Cianelli, D., Ciraolo, G., Corgnati, L., et al. (2022). Coastal high-frequency radars in the mediterranean–part 1: Status of operations and a framework for future development. Ocean science, 18(3):761–795.

Millot, C. (1999). Circulation in the western mediterranean sea. Journal of Marine Systems, 20(1-4):423–442.

Pinot, J.-M., Tintoré, J., and Gomis, D. (1995). Multivariate analysis of the surface circulation in the balearic sea. Progress in Oceanography, 36(4):343–376.

Saviano, S., Kalampokis, A., Zambianchi, E., and Uttieri, M. (2019). A year-long assessment of wave measurements retrieved from an hf radar network in the gulf of naples (tyrrhenian sea, western mediterranean sea). Journal of Operational Oceanography, 12(1):1–15.

Toste, R., Böck, C. S., da Silva, M. S., Moraes, N. O., Soares, A. E., Nehme, D. M., de Freitas Assad, L. P., Landau, L., Barreto, F., and da Silva Júnior, C. L. (2024). Codar data assimilation into an integrated ocean forecasting system for the brazilian southeastern coast. Ocean Modelling, 188:102331.

Vesecky, J. F. and Laws, K. E. (2010). Identifying ship echoes in codar hf radar data: A kalman filtering approach. In OCEANS 2010 MTS/IEEE SEATTLE, pages 1–8. IEEE.

Waskom, M. L. (2021). seaborn: statistical data visualization. Journal of Open Source Software, 6(60):3021.